

# The Cluster AgeS Experiment (CASE).<sup>†</sup> Variable stars in the field of the globular cluster M22<sup>\*</sup>

M. R o z y c z k a<sup>1</sup>, I. B. T h o m p s o n<sup>2</sup>, W. P y c h<sup>1</sup>,  
W. N a r l o c h<sup>1</sup>, R. P o l e s k i<sup>3</sup>  
and A. S c h w a r z e n b e r g – C z e r n y<sup>1</sup>

<sup>1</sup>Nicolaus Copernicus Astronomical Center, ul. Bartycka 18, 00–716 Warsaw,  
Poland

e-mail: (mnr, pych, wnarloch, alex)@camk.edu.pl

<sup>2</sup>The Observatories of the Carnegie Institution for Science, 813 Santa Barbara  
Street, Pasadena, CA 91101, USA

e-mail: ian@obs.carnegiescience.edu

<sup>3</sup> Department of Astronomy, Ohio State University, 140W. 18th Ave.,  
Columbus, OH43210, USA

e-mail: rpoleski@astrouw.edu.pl

## ABSTRACT

The field of the globular cluster M22 (NGC 6656) was monitored between 2000 and 2008 in a search for variable stars. *BV* light curves were obtained for 359 periodic, likely periodic, and long-term variables, 238 of which are new detections. Thirty nine newly detected variables, and 63 previously known ones are members or likely members of the cluster, including 20 SX Phe, 10 RRab and 16 RRc-type pulsators, one BL Her-type pulsator, 21 contact binaries, and 9 detached or semi-detached eclipsing binaries. The most interesting among the identified objects are V112 – a bright multimode SX Phe pulsator, V125 – a  $\beta$  Lyr-type binary on the blue horizontal branch, V129 – a blue/yellow straggler with a W UMa-like light curve, located halfway between the extreme horizontal branch and red giant branch, and V134 – an extreme horizontal branch object with  $P=2.33$  d and a nearly sinusoidal light curve; all four of them are proper motion (PM) members of the cluster. Among nonmembers, a  $P=2.83$  d detached eclipsing binary hosting a  $\delta$  Sct-type pulsator was found, and a peculiar  $P=0.93$  d binary with ellipsoidal modulation and narrow minimum in the middle of one of the descending shoulders of the sinusoid. We also collected substantial new data for previously known variables; in particular we revise the statistics of the occurrence of the Blazhko effect in RR Lyr-type variables of M22.

*globular clusters: individual (M22) – stars: variables – stars: SX Phe – blue stragglers – binaries: eclipsing*

## 1 Introduction

M22 is projected against the Galactic bulge at  $l=9^{\circ}9$ ,  $b=-7^{\circ}6$ , in a substantially reddened region with  $E(B-V)$  varying between 0.26 mag and 0.39 mag across our field of view<sup>1</sup>. Core radius  $r_c$ , half-light radius  $r_h$ , tidal radius  $r_t$ ,  $[\text{Fe}/\text{H}]$  index, radial velocity, heliocentric distance  $d_{\odot}$ , and galactocentric distance  $d_G$  of the cluster are equal to 1'33, 3'36, 32'0, -1.70, -146.3 $\pm$ 0.2 km/s, 3.2 kpc and 4.9 kpc, respectively (Harris 1996, 2010 edition). Dotter et al. (2010) excluded M22 from their age survey "because it is known to harbor multiple

<sup>†</sup>CASE was initiated and for long time led by our friend and tutor Janusz Kaluzny, who prematurely passed away in March 2015.

<sup>\*</sup>Based on data obtained with the Swope telescope at Las Campanas Observatory.

<sup>1</sup>The extinction calculator at [http://ned.ipac.caltech.edu/help/extinction\\_law\\_calc.html](http://ned.ipac.caltech.edu/help/extinction_law_calc.html) was used

stellar populations”. Indeed, Lee (2016) suggests that it is a merger of two globular clusters (GCs) which occurred in a dwarf galaxy, subsequently accreted onto the Milky Way. This might explain differences in age estimations of M22, varying from 12–13 Gyr (Lee 2015, 2016) up to 14 Gyr (Marino et al. 2009).

M22 is classified as an old GC of Oosterhoff type II, and has a rich and long blue horizontal branch (BHB). The  $(N_{BHB} - N_{RHB}) / (N_{BHB} + N_{RHB} + N_{RR})$  index, where  $N_{BHB}$  is the number of BHB stars,  $N_{RHB}$  the number of red HB stars (located redward of the instability strip on the CMD), and  $N_{RR}$  the number of RR Lyr stars, is equal to  $0.97 \pm 0.1$ , one of the largest among GCs with a substantial population of RR Lyr pulsators (Kunder et al. 2013a, hereafter K13).

Even though M22 is one of the closest GCs to the Sun, factors like very strong contamination of its field by bulge stars, substantial differential extinction, and appreciable concentration ( $c = \log r_t / r_c = 1.38$ ; Harris 1996, 2010 edition) make it a rather challenging target for studies. The pre-CCD searches for variables, summarized by Clement et al. (2001; 2017 edition<sup>2</sup>) (hereafter C01-17), resulted in the detection of 43 objects. The targeted CCD surveys performed so far (Kaluzny & Thompson 2001, hereafter KT01; Pietrukowicz & Kaluzny 2003, hereafter PK03; K13, and Sahay, Lebzelter & Wood 2014) brought additional 56 discoveries, including two optical cataclysmic variables and a microlensing event (Pietrukowicz et al. 2005, 2012). Fourteen of these objects are listed by C01-17 as members or possible members of the cluster, including eight RR Lyr pulsators, one contact binary, and five semiregular variables.

Apart from normal stars, the cluster contains two millisecond pulsars (Lynch et al. 2011), and two candidate stellar-mass black holes (Strader et al. 2012). Finally, according to Kains et al. (2016) M22 provides the best chance to detect an intermediate-mass black hole via astrometric microlensing.

Our survey is a part of the CASE project (Kaluzny et al. 2005) conducted using telescopes of the Las Campanas Observatory, with an aim of increasing the inventory of variable objects in the field of M22. It completes the previous findings of KT01 (based on 76 frames obtained during one night on the du Pont telescope) and PK03 (based on 31 archival HST/WFPC2 frames, and necessarily limited to the central part of the cluster). Altogether we identified 283 periodic, likely periodic or long-term variables not cataloged by C01-17, of which 45 were independently found by Soszyński et al. (2016; hereafter S16) during the OGLE-IV survey of the Galactic bulge. In Section 2, we briefly report on the observations and explain the methods used to calibrate the photometry. Newly discovered variables are presented and discussed in Section 3. Section 4 contains new data on previously known variables which we consider worthy of publishing, and the paper is summarized in Section 5.

## 2 Observations and data processing

Our paper is based on images acquired with the 1.0-m Swope telescope equipped with the  $2048 \times 3150$  SITe3 camera. The field of view was  $14.8 \times 22.8$  arcmin<sup>2</sup> at a scale of 0.435 arcsec/pixel. Observations were conducted on 86 nights from April 11, 2000 to August 22, 2008; always with the same set of filters. A total of 2730 *V*-band images and 384 *B*-band images were selected for the analysis. The seeing ranged from  $1''.2$  to  $3''.6$  and  $1''.2$  to  $3''.9$  for *V* and *B*, respectively, with median values of  $1''.4$  in both filters.

<sup>2</sup><http://www.astro.utoronto.ca/~cclement/cat/C0100m711>

The photometry was performed using an image subtraction technique implemented in the DIAPL package.<sup>3</sup> To reduce the effects of PSF variability, each frame was divided into  $4 \times 6$  overlapping subframes. The reference frames were constructed by combining 18 images in  $V$  and 17 in  $B$  with an average seeing of  $1.''1$  and  $1.''2$ , respectively. The light curves derived with DIAPL were converted from differential counts to magnitudes based on profile photometry and aperture corrections determined separately for each subframe of the reference frames. To extract the profile photometry from reference images and to derive aperture corrections, the standard Daophot, Allstar and Daogrow (Stetson 1987, 1990) packages were used. Profile photometry was also extracted for each individual image, enabling useful photometric measurements of stars which were overexposed on the reference frames.

## 2.1 Calibration

The photometric calibration is based on standard magnitudes and colors derived by KT01. Using over 40,000 comparison stars common to our survey and theirs, the following transformation to the standard system was derived:

$$\begin{aligned} V &= v + 2.0763(2) + 0.0191(2) \times (b - v) \\ B - V &= -0.1504(3) + 1.0400(3) \times (b - v), \end{aligned}$$

where lower case and capital letters denote instrumental and standard magnitudes, respectively, and numbers in parentheses are uncertainties of last significant digits.

Crowding in the field of view resulted in enhanced blending, which in turn significantly increased the scatter of photometric measurements in the observed magnitude range. For example, observations made of the globular cluster NGC 3201 (using the same instrument setup) resulted in a smallest scatter of 0.1 mag at  $V = 21$  mag (Kaluzny et al. 2016), while for M22 the best photometric accuracy is  $\sim 0.23$  mag (Fig. 1) at the same brightness level. Fig. 2, shows the CMD of the observed field and was constructed based on the reference images. To make the figure readable, only stars with measured proper motions (Narloch et al. 2017; hereafter N17) are selected to serve as a background for the variables. Stars identified as proper-motion (PM) members of the cluster are shown in the right panel.

## 2.2 Search for variables

The search for periodic variables was conducted using the AOV and AOV-TRANS algorithms implemented in the TATRY code (Schwarzenberg-Czerny 1996 and 2012; Schwarzenberg-Czerny & Beaulieu 2006). We examined time-series photometric data of 132,457 stars brighter than  $V \sim 22$  mag. The photometric accuracy was partly offset by the large number of available frames, and as a result we were able to detect periodic signals with amplitudes of  $\sim 0.02$  mag down to  $V \approx 15$  mag, and  $\sim 0.1$  mag down to  $V \approx 21$  mag.

Among the known variables within our field of view, light curves were obtained for all 45 stars discovered by S16, and for 76 out of 85 C01-17 stars. Of the latter, light curves are missing for SLW-7 which was overexposed in our frames, and for seven PK03 stars located close to the center of the cluster. We identified 238 new variable or likely variable stars, 36 of which are PM-members or likely

<sup>3</sup>Available from <http://users.camk.edu.pl/pych/DIAPL/index.html>

PM-members of M22. Membership status was also assigned to the variables known before. <sup>4</sup>

### 3 The new variables

Basic data for selected variables not listed in C01-17 are given in Table 1. For our naming convention to agree with that of C01-17 we start numbering the new variable cluster members from V102. The remaining variables are given names from U01 on (stars for which no PM-data are present) and from N01 on (stars whose PM indicates that they do not belong to M22). The equatorial coordinates in columns 2 and 3 conform to the UCAC4 system (Zacharias et al. 2013), and are accurate to  $0''.2 - 0''.3$ . The  $V$ -band magnitudes in column 4 correspond to the maximum light in the case of eclipsing binaries; in the remaining cases the average magnitude is given. Columns 5-7 give  $B - V$  color, amplitude in the  $V$ -band, and period of variability. A CMD of M22 with locations of the variables is shown in Fig. 3. Field objects are marked in black, those for which the PM data are missing or ambiguous in blue, and members of the cluster in red. The gray background stars are the PM-members of M22 from the right panel of Fig. 2.

#### 3.1 Members and likely members of M22

Based on proper motions, distances from the center of the cluster, and CMD locations we identified 39 M22-members not cataloged by C01-17 (among them, three discovered by S16). A star was considered a member or likely member if one of the following criteria was fulfilled:

1. PM-membership probability  $P_{PM} \geq 70\%$ .
2.  $P_{PM} < 70\%$ , but CMD-location compatible with cluster membership, variability type compatible with CMD-location, and geometric membership probability  $P_{geom} = 1 - \pi r^2 / S > 90\%$ , where  $r$  is star's distance from the center of M22 ( $\alpha = 18^{\text{h}} 36^{\text{m}} 23^{\text{s}}.94$ ,  $\delta = -23^{\circ} 54' 17''.1$ ) in arcseconds, and  $S = 1.22 \times 10^6$  is the size of the field of view in arcseconds<sup>2</sup> (there are two such cases).
3. Proper motion not known, but  $P_{geom} > 70\%$ , CMD-location compatible with cluster membership, and variability type compatible with CMD-location.

Details concerning PM measurements and calculations of membership probability are given in N17, who also provide a PM catalog for nearly 450000 stars in the fields of 12 GCs. In the following, we describe the ten most interesting variables, whose light curves are shown in Fig. 5.

Our data suggest that multimode pulsations are likely in 16 SX Phe stars (seven new ones and nine from the C01-17 catalog). The most interesting one among them is the newly detected variable V112, which is also the brightest and reddest blue straggler (BS). It clearly exhibits multimode pulsations at an amplitude of  $\sim 0.3$  mag suitable for asteroseismology analysis which in turn would provide valuable information on BS mass. Admittedly, its CMD location may seem a bit extreme for this type of variability, however both the  $V$  and  $B$

<sup>4</sup>Data for all the identified variables are available at <http://case.camk.edu.pl>

lightcurves are of good quality, so that a large error in  $\langle B \rangle - \langle V \rangle$  can be excluded.  $P_{PM}=100\%$  for V112, however we feel a radial velocity measurement would be necessary to confirm its membership. The star is a component of a blend. However, in the archival HST frame NGC6656-J9L948010 V112 is much brighter than the remaining components (in fact, it is strongly overexposed).

V116, a sinusoidal variable on the lower main sequence, is a 100% PM-member of M22. Our light curve is of poor quality because of partial blending with a much brighter star  $\sim 1''.5$  distant. We did not detect any periodicity in the latter, and V116 is well isolated in the archive HST frame NGC6656-U2X80302T. Thus, if the weak periodic signal we observe is real, then it must originate in V116 (not being entirely sure about its reality, we marked the star as a suspected variable). V116 would then closely resemble the optical counterpart of the X-ray source CX1 in M4 (Kaluzny et al. 2012).

V117 is a low-amplitude sinusoidal variable with a short period (0.31 d) clearly incompatible with its location on the red giant branch (RGB). However, it is a 100% PM-member of M22. Our image of V117 is perfectly symmetric, but, since the star is located in the unobserved by HST part of the cluster, the possibility of blending cannot be excluded. If adaptive optics photometry confirmed that we deal with a single light source, V117 would become an interesting target for further research.

V125, located on the blue horizontal branch (BHB), has a  $\beta$  Lyr-type (EB) light curve with minima of different depths, and  $P_{PM}=100\%$ . No HST data are available for this object. The star is well separated from its neighbors; nevertheless adaptive optics would be needed to exclude blending. If not a blend, V125 would be one of the very rare BHB binaries with short periods (Heber 2016).

V129, a BS with  $P_{PM}=100\%$ , which exhibits a W UMa-like (EW) light curve with minima of different depth, is peculiar because of its long period (1.39 d). The observed minima are broader than the maxima, also not fitting a W UMa interpretation. In our frame, variable V129 is blended with at least two fainter stars; unfortunately their contribution to the total light cannot be estimated because of lacking HST data.

The blue stragglers V130 and V131 are Algol-type eclipsing (EA) binaries with a strong ellipsoidal effect. No large observational effort would be needed to obtain reasonable quality light and velocity curves for these systems, and determine their parameters. Such a project would be worthwhile, as BS Algols provide a very demanding test suite for stellar evolution codes even in cases when their parameters are not accurately known (Stępień, Pamyatnykh & Rozycka 2017).

V133 is a detached eclipsing binary with a period ambiguity.  $P_1=2.244228$  d in Table 1 is the best fit to the light curve, with only one minimum visible. For  $P_2=1.195288$  d a secondary minimum appears, which may be as deep as the primary minimum. However, the fit becomes markedly poorer. Since PM is not available for V133, and  $P_{geom}=90\%$ , V133 is just a likely member of M22; potentially interesting since it might serve as age and distance indicator if its membership were confirmed. If it belongs to M22, the absence of the second minimum speaks against  $P_1$ , as the system is located too high above the lower main sequence for such a large luminosity difference between the components.

V134 is a nearly sinusoidal variable discovered by S16 (their star OGLE-BLG-ECL-423136). With  $P_{PM}=100\%$ ,  $P=2.33$  d, and a location between the extreme horizontal branch (EHB) and the BS region on the CMD, it constitutes a real puzzle. The high quality  $B$  and  $V$  light curves yield a reliable  $\langle B \rangle - \langle$

$V >$ , so that the chance that V134 is horizontally misplaced in the CMD is low. The most natural cause of this type of variability is a strong reflection effect similar to that observed in HW Vir binaries, however the period of V134 (2.331 d) is much longer than the longest period known among the members of that class ( $\sim 0.75$  d; Heber 2016). A slight elongation of the image of this star in our frames suggests a tight blend; unfortunately no HST data are available. Clearly, a spectroscopic follow-up is needed to verify its membership and reveal its nature.

V135, another detached eclipsing binary with a 1:2 period ambiguity, is located on the lower main sequence.  $P=4.928$  d and  $P=2.464$  d fit the lightcurve almost equally well; however the longer period implies nearly the same brightness of the components, which is barely compatible with the CMD location of the system. Thus, although V135 is a 100% PM-member of M22, its membership should be verified through radial velocity measurements.

### 3.2 Stars of unknown PM-membership

In our sample, there are 69 variables with  $P_{geom} < 70\%$  and unknown proper motions, at least some of which may turn out to belong to M22. Below we describe eight of the most interesting cases, whose light curves are shown in Fig. 6.

Algos U39 (OGLE-BLG-ECL-423130) and U53 are prospective yellow stragglers. If their membership is confirmed they will provide excellent opportunity to test and/or calibrate stellar evolution codes (Stępień, Pamyatnykh & Rozycka 2017).

U44 is a RS CVn-type eclipsing binary with a strong sinusoidal modulation, resembling V9 in NGC 6971 (Kaluzny 2003; Bruntt et al. 2003) or a sample of RS CVn discovered within the OGLE III survey and described by Pietrukowicz et al. (2013). Only one eclipse is visible, situated almost in the middle of the ascending branch of the light curve. The modulation originates from spot(s) possibly accompanied by mass transfer effects, similarly to those observed in R Ara (Bakiş et al. 2016). Since such systems are rare, a follow-up of U44 would be desirable independently of its membership status.

U50 and U61 are detached eclipsing binaries located to the right of the lower main sequence. Both their light curves reveal only one eclipse. If follow-up photometry confirms our light curve fits, the systems would become interesting red straggler candidates (see e.g. Kaluzny 2003).

U51, a detached eclipsing binary with two eclipses visible, has a period long enough (2.6 d) to serve as age and distance indicator despite its low brightness.

U56, located redward of the subgiant branch, is another red straggler candidate.

U62 is a detached eclipsing binary located on the subgiant branch, and another potential excellent age and distance indicator. As our light curve covers only a part of a single eclipse, its period of 20.8d is only tentative.

### 3.3 Field variables

We identified 176 variables which according to N17 do not belong to M22. As errors in PM measurements cannot be entirely excluded, a few of them may in principle turn out to be cluster members. For that reason, while selecting the most interesting cases, we paid special attention to stars located on the CMD in

the vicinity of the turnoff or in the BS region. The light curves of the selected variables are shown in Fig. 7.

N04, N10, and N11 are either field  $\delta$  Sct variables or cluster SX Phe stars and blue stragglers, all showing clear multimode pulsations.

N12, a clear multimode pulsator located in the RR Lyr gap, has a period of only 0.15 d, which unambiguously identifies it as a field  $\delta$  Sct star.

N15, located in the BS region, is another multimode pulsator. Its period of 0.25 d is too long for a SX Phe variable; therefore it must also be a field  $\delta$  Sct star.

N44 is a field contact binary with a variable light curve. Its brightness seems to have decreased by  $\sim 0.08$  mag between 2000 and 2008 (the 2008 data were collected during four nights, so that a zero point artefact is rather unlikely – the more that such effects are not seen in any other lightcurve).

N65 (OGLE-BLG-ECL-423254) is a W UMa eclipsing binary in poor thermal contact. The secondary eclipse is total, allowing an estimation of the temperature of the primary from the color–temperature calibration. The observed  $B - V$  index is 0.70 mag. Assuming a reddening of 0.30 mag (an average for M22) and using the calibration of Sousa et al (2011) one obtains  $T_1 = 6500$  K. An approximate solution of the  $V$ - and  $B$ -band light curves with the PHOEBE implementation of the Wilson–Devinney code (Prša and Zwitter 2005) yields  $i = 85^\circ 8$ ,  $T_2 = 4400$  K, and  $\Delta M_{bol} = 2.9$  mag between the components. Neglecting the contribution of the secondary, and assuming that N65 is a member of M22, from the observed  $V = 17.85$  mag at maximum light, we obtain  $M_{bol}^1 = 4.38$  mag. This absolute brightness is reproduced by a W–D solution with semimajor axis and mass of the primary of  $2 R_\odot$  and  $0.25 M_\odot$ , respectively. Since the latter value is much too low for a 6500 K star, N65 must be a background object, only interesting because of the significant temperature difference between the components.

N87 seems similar to U44, however there is a significant difference between them: N88 has two maxima per period instead of one. Since a configuration of two nearly identical spots at locations differing by nearly  $180^\circ$  in longitude is rather unlikely, the nature of N88 is puzzling; the more that a similar object, OGLE-GD-ECL-04649, mentioned by Pietrukowicz et al. (2013), exhibits both a single and a double maximum at various seasons. The double-peaked curve resembles that of a cataclysmic variable with a giant donor (e.g. T CrB) yet the color is 1 mag too red. The system clearly deserves thorough follow-up observations, especially since it is just 1.4 arcsec distant from the Chandra X-ray source C183656.05-234845.5 with  $(\alpha, \delta)_{2000} = (279.23355, -23.81263)$ .

N107 is a detached eclipsing binary, interesting independently of its membership status, since it hosts a  $\delta$  Sct or SX Phe star. In Fig. 7 the light curve of this system is phased separately with the pulsation period (0.08 d) and with the orbital period (2.83 d).

Another two detached systems, N113 (OGLE-BLG-ECL-423112) and N121, are potentially interesting because of their CMD locations near the bottom of the red giant branch. If either of these turns out to be M22 member, it would provide a good reference point for isochrone fitting in  $M - R$  and  $M - L$  diagrams (see e.g. Kaluzny et al. 2013).

## 4 New data on known variables

Of the 101 objects cataloged by C01-17 fourteen are located beyond our FOV, and two are pulsars without optical counterparts. Due to crowding and blending, among the eight variables discovered by PK03 in HST frames of the central part of M22 only PK-05 could have been identified (all star designations in this Section are taken from C01-17). For the remaining 78 stars membership status and membership probability were assigned using the criteria given in Section 3.1. Stars #3, #14, #39, #40, KT-01, KT-03, KT-05, KT-15, KT-18, KT-40, KT-41 and KT-48 turned out to be field objects.

There are 10 RRab and 16 RRc pulsators in M22. A detailed analysis of our data on these objects will be published elsewhere; here we limit ourselves to a general remark concerning the Blazhko effect. K13 suggest a small incidence ( $\sim 10\%$ ) of the Blazhko effect among RRab stars of M22, and do not detect any such effects in stars of RRc type. In fact, the only star with a firmly established Blazhko effect they report is KT-55. We observe this behavior also in RRab stars #2, #3 and #6. Another RRab star, #23, suggested by K13 to have a rapidly changing or erratic period, does not show any such changes in our data: we only observe modest ( $\pm 0.05$  mag) variations of the descending shoulder of the light curve, which in principle might be interpreted as a weak Blazhko effect. Thus, according to our data, the incidence of the Blazhko effect among RRab stars is 40% (50% if #23 is included). Moreover, we find a Blazhko effect of a varying strength in RRc stars #18, #19, #25 and KT-36 (phase), #15 (phase, shape) and KT-26, KT-37, Ku-1, Ku-2, Ku-3 and Ku-4 (phase, shape, amplitude). Altogether, we observe Blazhko behavior for 15 (16) RR pulsators, i.e. an incidence rate of 58% (62%). Among the RRc stars the incidence is even higher – 68%. Thus, M22 is another GC with a large ( $>50\%$ ) percentage of RRc Blazhko behavior, joining NGC 2808 (Arellano Ferro et al. 2012) and M53 (Kunder et al. 2013b).

Below we briefly describe C01-17 stars listed in Table 2, whose light curves are shown in Fig. 8.

Star #24: To our surprise, this object, listed as a non-variable by K13, turns out to be a BL Her pulsator with  $P = 1.715$  d, and a stable lightcurve. Our data show no period doubling phenomenon foreseen theoretically by Buchler & Moskalik (1992), and for the first time observed by Smolec et al. (2012) in a star belonging to the Galactic bulge.

Star #31: In our data no star closer than  $5''$  to the position of #31 shows evidence for variability.

KT-02: This Algol-type binary star, relatively isolated within M22, and located slightly above the turnoff of the cluster, is a potentially valuable age and distance indicator (Kaluzny et al. 2005). KT01 observed the  $\sim 0.25$  mag deep secondary minimum only. We find the primary minimum to be  $\sim 0.4$  mag deeper, indicating not too discrepant temperatures of the components. Thus, spectral lines of both the components should be visible, and despite the short period ( $P=0.49$  d) the system is bright enough ( $V=17.35$  mag) for good quality spectra to be obtained and an accurate velocity curve to be extracted.

KT-26: The light curve of this star suggests that this is an RRc pulsator exhibiting the Blazhko effect. However, KT-26 is too blue to be an ordinary RRc star (both the  $V$  and  $B$  lightcurves are of very good quality, so that a large error in  $B-V$  is rather unlikely, the more that our  $V$ -band brightness agrees very well with that of K13). The archival Hubble frame NGC6656-J9L948010 reveals KT-26 is a  $\sim 0''.75$  blend of two stars with a flux ratio  $\sim 15:8$ . Unfortunately, since



this is the only available ACS frame taken in the F606W filter, one cannot tell which component of the blend is the proper variable. If the brighter one, then its brightness is lower by  $\sim 0.5$  mag than the combined brightness of the blend, and  $\sim 0.2$  mag lower than that of the weakest RR Lyr in M22 (i.e. star #23). In that case, the proper variable would resemble the peculiar pulsator V37 in NGC 6362 (Smolec et al. 2017). If the fainter component were variable, the magnitude difference would increase to  $\sim 1.2$  mag and  $\sim 0.9$  mag, respectively, moving it to the BHB. Then, however, its period of 0.361366 d would be definitely too long for a BHB star. In any case, KT-26 clearly deserves closer observational scrutiny.

KT-39: Tentatively classified by KT01 as a contact binary, this is in fact another interesting and potentially valuable Algol-type system. Its location just below the subgiant branch indicates that at least one of the components must have left the main sequence, thus providing a good point for isochrone fitting. With a difference between depths of minima similar to that of KT-02, comparable isolation and a period three times longer, KT-39 is a relatively easy target for spectroscopy.

KT-46: Another Algol-type binary. KT01 only observed the  $\sim 1$  mag deep primary minimum. We found the secondary minimum is more than ten times shallower, which together with a maximum brightness of  $V \sim 19.6$  mag and a period of only 0.61 d rather eliminates this system from the list of currently interesting objects. The light curve for KT-46 can be downloaded from the CASE archive.

KT-13, KT-20, KT-23, KT-33, KT-42 and KT-43 are contact binaries located at the turnoff or in the BS region (KT-42 was erroneously classified by KT01 as a possible pulsator). Another three contact binaries, KT-07, KT-08 and PK-05, occupy positions to the right of the lower main sequence. For all the eight binaries complete light curves are presented. All of them, including PK-05 which is placed closest to the center of M22, are well isolated within the cluster, so that radial velocity measurements seem entirely feasible (see Rozycka et al. 2010). KT-08 is particularly interesting as the first, and so far the only, contact binary found within CASE to reside significantly ( $\sim 2$  mag) below the turnoff of a globular cluster.

KT-51: This star, located at the top of the EHB, was singled out by KT01 as the most interesting object in their sample; possibly a binary. We confirm its variability, however with a different period than theirs (0.103 d vs.  $\sim 0.2$  d) and with a different amplitude (0.04 mag vs. 0.06 mag). Thus, the question of the binarity of this object remains open. In the archival HST/WFPC2 frame UA2L0802M, KT-51 is an unresolved blend  $\sim 0''.3$  wide.

## 5 Summary

This contribution substantially increases the inventory of variable stars in the field of M22. A total of 359 variables or suspected variables were detected, 238 of which had been not known before. 102 members or likely PM-members of the cluster were identified, including 20 SX Phe, 10 RRab and 16 RRC pulsators, one BL Her pulsator, 21 contact binaries, and 8 detached or semi-detached binaries. Periods were obtained for almost all of the observed variables except a few cases with variability timescale longer than our time base.

Among the new members of M22, the most interesting objects for follow-up studies are V125 – a  $\beta$  Lyr-type BHB binary, V129 – a blue/yellow straggler

with a W UMa-like light curve located halfway between EHB and RGB, and V134 – an EHB object with  $P = 2.33$  d and sinusoidal light curve. Among nonmembers, observational scrutiny would be desirable for N107 – a detached eclipsing binary hosting a  $\delta$  Sct-type pulsator, N44 – a contact binary whose luminosity seems to have decreased by 0.08 mag between 2000 and 2008, and N87 – a peculiar  $P = 0.93$  d binary with ellipsoidal modulation and narrow minimum in the middle of one of the descending shoulders of the sinusoid which may be an optical counterpart of the Chandra X-ray source C183656.05-234845.5. Multimodality was detected in 16 SX Phe stars, with the blue straggler V112 being the most prominent example of this type of variability.

We also provide substantial new data on the variables cataloged by C01-17. In particular, we identify M22 as the third GC with a large ( $>50\%$ ) percentage of Blazhko effect incidence among RRc stars after NGC 2808 (Arellano Ferro et al. 2012) and M53 (Kunder et al. 2013b). The RRc star KT-26 shows a peculiar behaviour, resembling that found for V37 in NGC 6362 by Smolec et al. (2017). Finally, the contact binary KT-08 is the first, and so far the only such system found within CASE to reside significantly ( $\sim 2$  mag) below the turnoff of a globular cluster. As such, it might provide some constraints on the evolution of binary systems in GCs.

**Acknowledgements.** We thank Grzegorz Pojmański for the lc code which vastly facilitated the work with light curves, and to the anonymous referee for many comments and suggestions which substantially improved the manuscript. This paper is partly based on data obtained from the Mikulski Archive for Space Telescopes (MAST). STScI is operated by AURA, Inc., under NASA contract NAS5-26555. Support for MAST for non-HST data is provided by the NASA Office of Space Science via grant NNX09AF08G and by other grants and contracts.

## REFERENCES

- Arellano Ferro, A., Bramich, D. M., Figuera Jaimes, R., Giridhar, S., and Kuppuswamy, K. 2012, *MNRAS*, **420**, 1333.
- Bakiş, H., Bakiş, W., Eker, Z., and Demircan, O. 2016, *MNRAS*, **458**, 508.
- Bruntt, H., Grundahl, F., Tingley, B., Frandsen, S., Stetson, P. B., and Thomsen, B. 2003, *Astron. Astrophys.*, **410**, 323.
- Buchler J. R., and Moskalik, P. 1992, *Astrophys. J.*, **391**, 736.
- Clement, C. M., Muzzin, A., Dufton, Q., Ponnampalam, T., Wang, J. et al. 2001, *Astron. J.*, **122**, 2587 (C01-17).
- Dotter, A., Sarajedini, A., Anderson, J., Aparicio, A., Bedin, L. R. et al. 2010, *ApJ*, **708**, 698.
- Harris, W.E. 1996, *Astron. J.*, **112**, 1487.
- Heber, U. 2016, *P.A.S.P.*, **128**, 082001.
- Kains, N., Bramich, D. M., Sahu, K. C., and Calamida, A. 2016, *MNRAS*, **460**, 2025.
- Kaluzny, J. 2000, *ASP Conf.Ser.*, **203**, 19.
- Kaluzny, J. 2003, *Acta Astron.*, **53**, 51.
- Kaluzny, J., and Thompson, I. B. 2001, *Astron. Astrophys.*, **373**, 899 (KT01).
- Kaluzny, J., Thompson, I. B., Krzeminski, W., Preston, G. W., Pych, W. et al. 2005, *Stellar Astrophysics with the World's Largest Telescopes, AIP Conf. Proc.*, **752**, 70.
- Kaluzny, J., Rozanska, A., Rozyczka, M., Krzeminski, W., and Thompson, I. B. 2012, *Astrophys. J.*, **750L**, 3.
- Kaluzny, J., Thompson, I. B., Rozyczka, M., Dotter, A., Krzeminski, W. et al. 2013, *Astron. J.*, **145**, 43.
- Kaluzny, J., Rozyczka, M., Thompson, I. B., Narloch, W., Mazur, B. et al. 2016, *Acta Astron.*, **66**, 31.
- Kunder, A., Stetson, P. B., Cassisi, S., Layden, A., Bono, G. et al. 2013a, *Astron. J.*, **146**, 119. (K13)
- Kunder, A., Stetson, P. B., Catelan, M., Walker, A., and Amigo, P. 2013b, *Astron. J.*, **145**,

- 33.
- Lee, J-W. 2015, *Astrophys. J. Suppl. Ser.*, **219**, :7.
- Lee, J-W. 2016, *Astrophys. J. Suppl. Ser.*, **226**, :16.
- Lynch, R. S., Ransom, S. M., Freire, P. C. C., and Stairs, I. H. 2011, *Astrophys. J.*, **734**, 89.
- Marino, A. F., Milone, A. P., Piotto, G., Villanova, S., Bedin, R. L. et al. 2009, *Astron. Astrophys.*, **505**, 1099.
- Mazur, B., Krzeminski, W., and Thompson, I. B. 2003, *MNRAS*, **340**, 1205.
- Narloch, W., Kaluzny, J., Poleski, R., Rozycka, M., Pych, W., and Thompson, I. B. 2017, *MNRAS*, **471**, 1446. (N17)
- Nemec, J. M., Balona, L. A., Murphy, S. J., Kinemuchi, K., and Jeon, Y.-B. 2017, *MNRAS*, **466**, 1290.
- Petersen J. O., and Christensen-Dalsgaard J. 1996, *Astron. Astrophys.*, **312**, 463.
- Pietrukowicz, P., and Kaluzny, J. 2003, *Acta Astron.*, **53**, 371 (PK03).
- Pietrukowicz, P., Kaluzny, J., Thompson, I. B., Jaroszynski, M., Schwarzenberg-Czerny, A. et al. 2005, *Acta Astron.*, **55**, 261.
- Pietrukowicz, P., Minniti, D., Jetzer, Ph., Alonso-García, J., and Udalski, A. 2012, *Astrophys. J. Letters*, **744**, 18.
- Pietrukowicz, P., Mróz, P., Soszyński, I., Udalski, A., Poleski, R. et al. 2013, *Acta Astron.*, **63**, 115.
- Prša, A., and Zwitter, T. 2005, *Astrophys. J.*, **628**, 426.
- Rozycka, M., Kaluzny, J., Pietrukowicz, P., Pych, W., Catelan, M. et al. 2010, *Astron. Astrophys.*, **524**, 78.
- Sahay, A., Lebzelter, T., and Wood, P. R. 2014, *Publ. Astr. Soc. Austr.*, **31**, 12.
- Saio, H., Kurtz, D. W., Takata, M., Shibahashi, H., Murphy, S. J. et al. 2015, *MNRAS*, **443**, 3264.
- Schwarzenberg-Czerny, A. 1996, *Astrophys. J. Letters*, **460**, L107.
- Schwarzenberg-Czerny, A. 1999, *Astrophys. J.*, **516**, 315.
- Schwarzenberg-Czerny, A. 2012, *New Horizons in Time-Domain Astronomy, IAU Symposium*, **285**, 81.
- Schwarzenberg-Czerny A., and Beaulieu, J.-Ph. 2006, *MNRAS*, **365**, 165.
- Smolec, R., Moskalik, P., Kauny, J., Pych, W., Ryczka, M., and Thompson, I. B. 2017, *MNRAS*, **467**, 2349.
- Smolec, R., Soszyński, I., Moskalik, P., Udalski, A., Szymański, M. K. et al. 2012, *Astrophys. & Sp. Sci. Proc*, **31**, 85.
- Soszyński, I., Pawlak, M., Pietrukowicz, P., Udalski, A., Szymański, M. K. et al. 2016, *Acta Astron.*, **66**, 405 (S16).
- Sousa, S. G., Alapini, A., Israelian, G., and Santos, N. C. 2010, *Astron. Astrophys.*, **512**, 13.
- Stępień, K., Pamyatnykh, A. A., and Rozycka, M 2017, *Astron. Astrophys.*, **587**, 87.
- Stetson, P. B. 1987, *P.A.S.P.*, **99**, 191.
- Stetson, P. B. 1990, *P.A.S.P.*, **102**, 932.
- Strader, J., Chomiuk, L., Maccarone, T. J., Miller-Jones, J. C. A., and Seth, A. C. 2012, *Nature*, **490**, 71.
- Zacharias, N., Finch, C. T., Girard, T. M., Henden, A., Bartlett, J. L. et al. 2013, *Astron. J.*, **145**, 44.

## Appendix: V112 – a multi-mode, non-radial SX Phe type pulsating star

### 6.1 Light curve decomposition

The short period and unstable light curve of the blue straggler V112 suggests it to be a SX Phe type star. Cores of globular clusters host many such stars yet most appear to be of low amplitude (Kaluzny 2000; for recent references see Nemec et al. 2017). Because of its large amplitude V112 seemed worthy of further attention. We performed a complete Fourier decomposition of its light curve, employing the NFIT code by one of authors (ASC). For early application of this code to SX Phe light curves, and underlying methods, see Mazur et al. (2003), and Schwarzenberg-Czerny (1999), respectively. The analysis is performed in stages, so that consecutive frequencies are identified in the periodogram, and

subsequently data are prewhitened of them. In that way a Fourier model of the light curve is established. At the final stage the model is refined by fitting all frequency terms simultaneously by non-linear least squares, with adjustment of the base frequencies. The effective Nyquist interval of our observations is close to 130 c/d. Our decomposition of the light curve of V112 is *complete* in that we accounted for all frequencies in the range up to 100 c/d and with half-amplitudes over 0.0015 mag, i.e. twice their typical standard deviation ( $\sigma = 0.008$  mag). Even for these small amplitudes the standard deviation of phases remains within  $0.08P$  while for 9 strong modes they were  $\ll 0.01P$ .

## 6.2 Pulsation modes of V112

Our analysis revealed three base frequencies of pulsation,  $f_0, f_1$ , and  $f_2$ , with some harmonics and also seven combination frequencies between them (see Table 3). Hence it may be securely assumed all these frequencies correspond to the pulsation of V112. The ratio  $f_0/f_1 = 0.784$  is within the range of that for fundamental-to-first-overtone radial p-modes in SX Phe, depending on metallicity (e.g. Petersen & Christensen-Dalsgaard 1996), hence it seems secure to identify  $f_0$  and  $f_1$  with the fundamental and first overtone pulsation of V112. If so, the presence of the combination mode  $f_2 + f_0$  with  $f_2$  close to  $f_0$  constitutes evidence of a non-radial mode  $f_2$ .

In the light curve of V112, there appear another 3 seemingly unrelated frequencies  $f_3, f_4$ , and  $f_5$ . Note that  $f_3$  differs substantially from the combination  $2f_0 - 2f_2$  and its moon alias. It appears within a low frequency power bump at  $f < 2$  c/d. Such a bump does appear in some SX Phe candidate stars observed by Kepler Satellite (Nemec et al. 2017), and a coherent frequency found in Kepler data for a  $\delta$  Scuti star is interpreted as due to either stellar rotation or g-modes (Saio et al. 2015). Our ground-based mono-site data may suffer from a zero level drift for frequencies below 0.2 c/d (Mazur et al. 2003), though most of the low-frequency bump could be real, similar to the one in Kepler stars. The remaining frequencies  $f_4$  and  $f_5$  are ill-expressed in our data. Although their amplitudes reach 6 and  $4.5\sigma$ , an NLSQ fit yields as standard deviation as large as that corresponding to a  $0.1P$  uncertainty over a half time-span of our data. We leave the question of their reality and nature open.

Due to the simultaneous presence of well established fundamental and first overtone radial p-modes and a non-radial one, V112 belongs to a subgroup of SX Phe stars most suitable to an asteroseismic analysis. There are signs of the presence of low frequency  $f_3$  &  $f_4$  oscillations consistent with g-modes, yet due to their small amplitude and uncertain fits we refrain from further discussion. As  $f_0$  and  $f_0/f_1$  are tied to metallicity and luminosity, from such analysis of V112 it may be possible to get information on chemical composition and distance of M22 – the more that the presence of non-radial mode(s) yields additional constraints.

Table 1: Basic data of selected new variables discovered in the field of M22

ID	RA [deg]	DEC [deg]	V [mag]	B-V [mag]	$\Delta_V$ [mag]	Period [d]	Type <sup>a</sup>	Mem <sup>c</sup>
V112	279.10487	-23.90030	15.73	0.69	0.30	0.062316	SX	Y
V116	279.14455	-23.96458	19.74	1.16	0.13	0.166970	<i>susp</i>	Y
V117	279.06735	-23.93642	15.84	0.96	0.02	0.313255	<i>sin</i>	Y
V125	278.98951	-23.79977	14.52	0.19	0.02	0.542888	EB	Y
V129	279.08844	-23.86043	15.80	0.52	0.05	1.394800	EW	Y
V130	279.07328	-23.95401	16.63	0.61	0.04	1.445972	EA	Y
V131	279.10074	-23.90743	16.00	0.43	0.26	1.733622	EA	Y
V133	279.15541	-23.89410	18.99	1.10	0.24	2.244228	EA	Y
V134	279.06929	-23.93284	16.82	0.21	0.14	2.330917	<i>sin</i>	Y
V135	279.23132	-23.92565	18.79	0.79	0.16	4.927996	EA	Y
U39	279.06515	-23.97477	16.52	0.72	0.20	0.626613	EA	U
U44	278.97674	-24.06404	18.95	1.25	0.27	0.811103	RS CVn/E	U
U50	279.10452	-23.94817	18.29	1.15	0.11	1.922292	EA	U
U51	279.16651	-23.87156	19.67	0.89	0.44	2.548926	EA	U
U53	278.98998	-23.72693	16.70	0.78	0.61	4.148438	EA	U
U56	279.16653	-23.84856	17.09	1.08	0.13	4.572758	<i>per</i>	U
U61	279.22293	-23.78627	18.91	1.07	0.19	13.81400	EA	U
U62	278.99650	-23.91997	16.76	0.84	0.04	20.75220	EA	U
N04	279.11355	-23.79272	16.45	0.60	0.06	0.042513	SX/DSCT	N
N10	278.97078	-24.06584	15.35	0.52	0.05	0.089940	SX/DSCT	N
N11	279.11653	-23.82832	16.45	0.52	0.30	0.097236	DSCT	N
N12	279.14421	-24.01212	13.71	0.61	0.07	0.146750	DSCT	N
N15	279.20356	-24.03031	16.76	0.46	0.20	0.245619	DSCT	N
N44	278.99070	-23.75487	15.91	0.87	0.19	0.414372	EW	N
N65	279.21231	-24.04217	17.68	0.72	0.44	0.592321	EW	N
N87	279.23363	-23.81226	17.03	1.47	0.06	0.925052	?	N
N107	279.17496	-24.00387	16.82	0.51	0.09	0.078948	DSCT	N
N107	279.17496	-24.00387	16.82	0.51	0.17	2.831980	EA	N
N113	279.04831	-23.80348	17.23	0.91	0.20	3.997504	EA	N
N121	279.19535	-23.87185	16.73	0.87	0.25	6.068994	EA	N

<sup>a</sup> EA - detached eclipsing binary, EB - type  $\beta$ Lyr eclipsing binary, EW - contact binary, RS CVn/E - RS CVn-type binary with eclipse, SX - type SX Phe pulsator, DS - type  $\delta$  Sct pulsator, *sin* - sinusoidal light curve of unknown origin, *per* - periodic variable of unknown type, *susp* - suspected variable.

<sup>c</sup> Membership status: Y - member or likely member, U - no data or data ambiguous, N - field object.

Table 2: Basic data of C01-17 variables for which important new information is provided

ID <sup>a</sup>	RA [deg]	DEC [deg]	V [mag]	B - V [mag]	$\Delta_V$ [mag]	Period [d]	Type <sup>b</sup> Remarks <sup>c</sup>	Mem <sup>d</sup>
24	279.09078	-23.90371	13.42	0.90	0.65	1.714854	BL Her	Y
KT-02	279.17424	-23.93922	17.33	0.65	0.28	0.490629	EA/EB	Y
KT-07	279.15353	-23.95021	17.67	0.85	0.49	0.329797	EW	Y
KT-08	279.14863	-23.92095	19.68	1.08	0.64	0.363902	EW	Y
KT-13	279.12860	-23.89616	17.22	0.68	0.45	0.281733	EW	Y
KT-20	279.10869	-23.85749	16.66	0.44	0.17	0.288495	EW; BS	Y
KT-23	279.09932	-23.85456	16.47	0.43	0.24	0.298523	EW; BS	Y
KT-26	279.09650	-23.88985	14.04	0.28	0.21	0.361366	RRc; Bl	Y
KT-33	279.07025	-23.89847	16.96	0.72	0.08	0.244137	EW	Y
KT-39	279.04161	-23.86605	17.28	0.84	0.19	1.474834	EA	Y
KT-42	279.14445	-23.87534	17.29	0.62	0.11	0.554893	EW; BS	Y
KT-43	279.10116	-23.93863	17.36	0.77	0.10	0.220520	EW	Y
KT-46	279.09066	-23.97364	19.41	0.92	0.99	0.610198	EA	Y
KT-51	279.14617	-23.88433	14.62	0.20	0.015	0.103422	sin; BHB	Y
PK-05	279.09275	-23.90914	18.31	0.92	0.25	0.242839	EW	Y

<sup>a</sup> After C01-17.

<sup>b</sup> EA - detached eclipsing binary, EB - type  $\beta$ Lyr eclipsing binary, EW - contact binary, BL Her - type BL Her pulsator, RRc - type RRc pulsator, sin - sinusoidal light curve of unknown origin.

<sup>c</sup> Bl - Blazhko effect, BHB - blue horizontal branch object, BS- blue straggler.

<sup>d</sup> Membership status: Y - member or likely member.

Table 3: Pulsation frequencies in V112

Frequency[c/d]	Amplitude <sup>a)</sup>	Type
16.0472041	0.1195	$f_0(F)$
32.0944082	0.0440	$2f_0$
20.4731506	0.0285	$f_1(1 OT)$
4.4259466	0.0190	$f_1 - f_0$
36.5203547	0.0185	$f_1 + f_0$
48.1416123	0.0180	$3f_0$
11.6212575	0.0135	$2f_0 - f_1$
64.1888164	0.0102	$4f_0$
52.5675588	0.0098	$2f_0 + f_1$
1.2720596:	0.0076:	$f_3$
68.6147629	0.0070	$3f_0 + f_1$
15.3964482	0.0069	$f_2(NR)$
27.6684616	0.0052	$3f_0 - f_1$
31.4436523	0.0049	$f_0 + f_2$
6.0188051:	0.0048:	$f_4$
84.6619670	0.0043	$4f_0 + f_1$
80.2360205	0.0039	$5f_0$
91.9997502:	0.0037:	$f_5$
96.2832246	0.0027	$6f_0$
112.3304287	0.0020	$7f_0$
40.9463013	0.0017	$2f_1$
61.4194519	0.0015	$3f_1$
81.8926026	0.0014	$4f_1$
128.3776328	0.0014	$8f_0$

<sup>a</sup> Half peak-to-peak amplitude in magnitudes

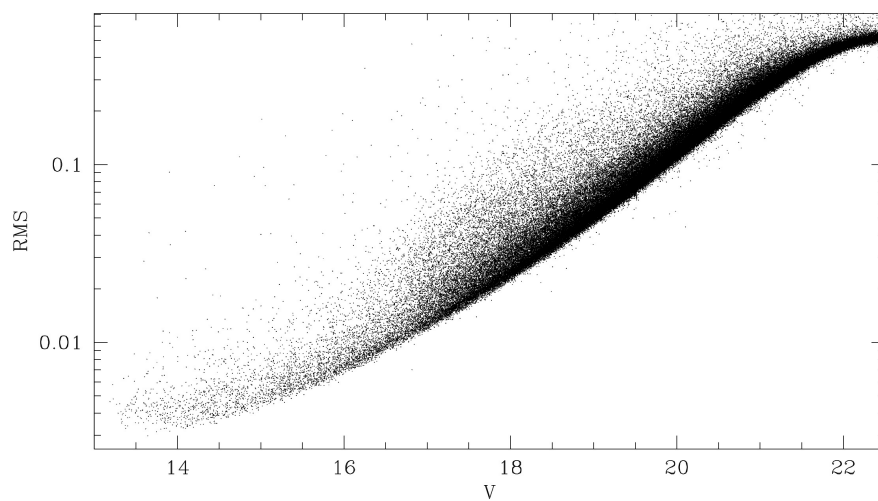


Figure 1: Standard deviation vs. average  $V$ -band magnitude for light curves of stars from the M22 field.

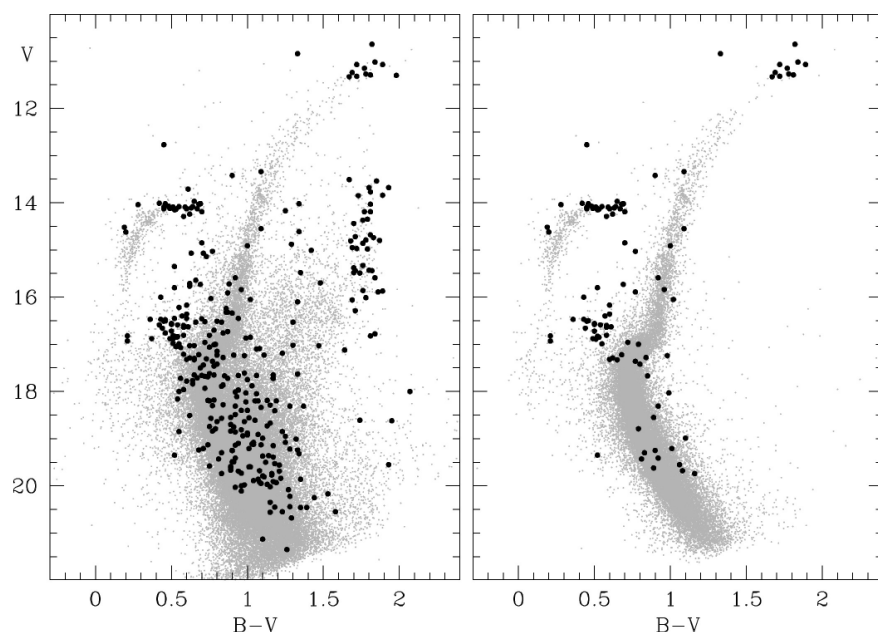


Figure 2: CMD for the observed field. Left: all stars for which proper motions were measured. Black points mark all the variables detected within the present survey for which  $B$ -band magnitudes were available. Right: same as in the left panel, but for PM-members of the cluster only.

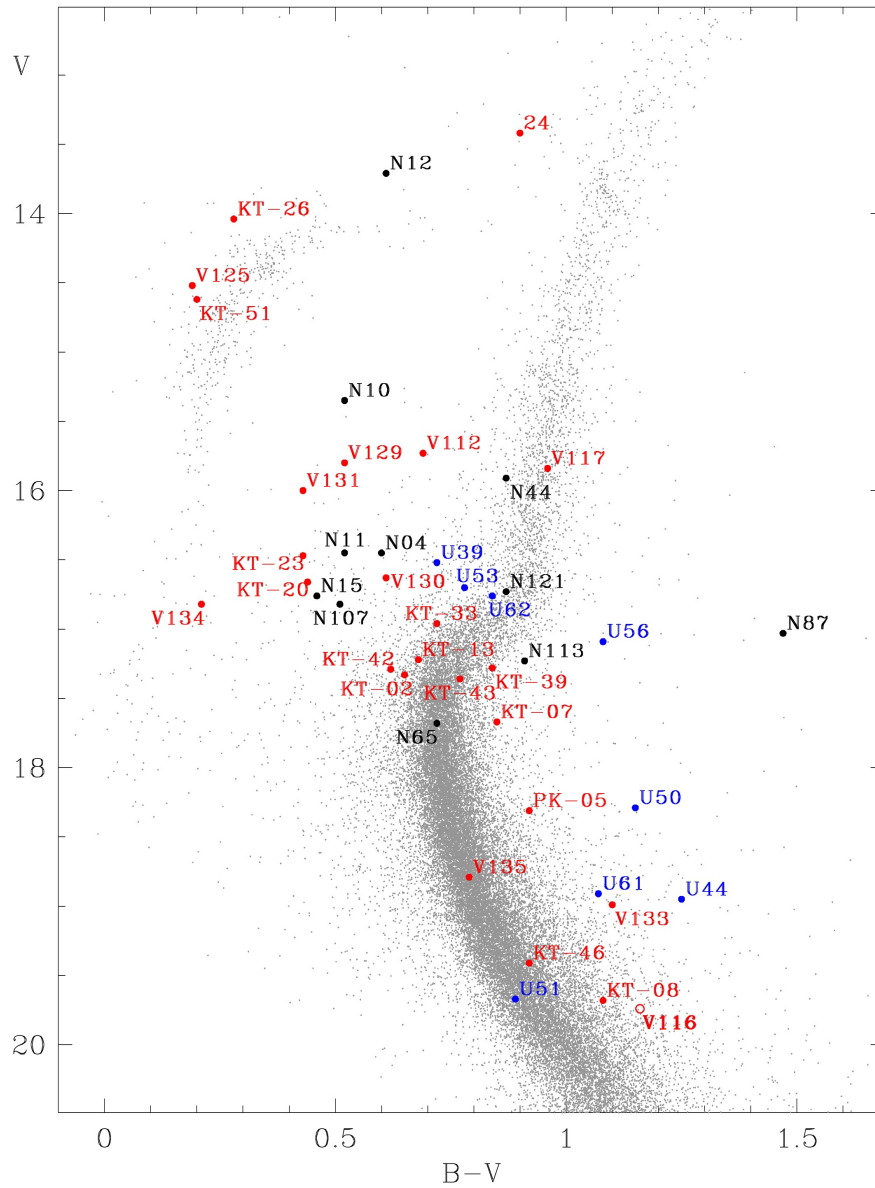


Figure 3: CMD for the observed field with locations of the variables described in Sections 3 and 4 (to make the figure readable, the remaining variables identified within the present survey are not shown). Red: PM-members of M22; blue: stars for which PM-data are missing; black: field stars. Filled circles: confirmed variables; open circle: suspected variable. The gray background stars are the same as in the right panel of Fig. 2.



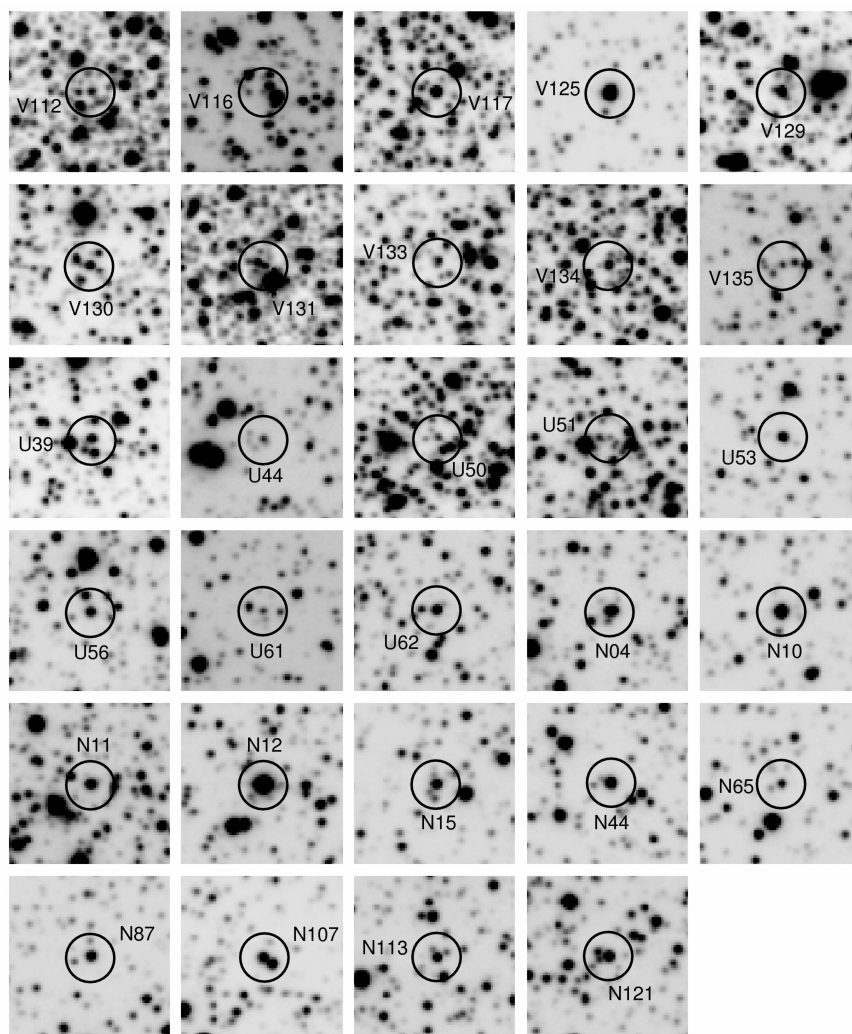


Figure 4: Finding charts for the new variables whose light curves are shown in Figs. 5, 6, and 7. Each chart is 30'' on a side. North is up and East to the left.

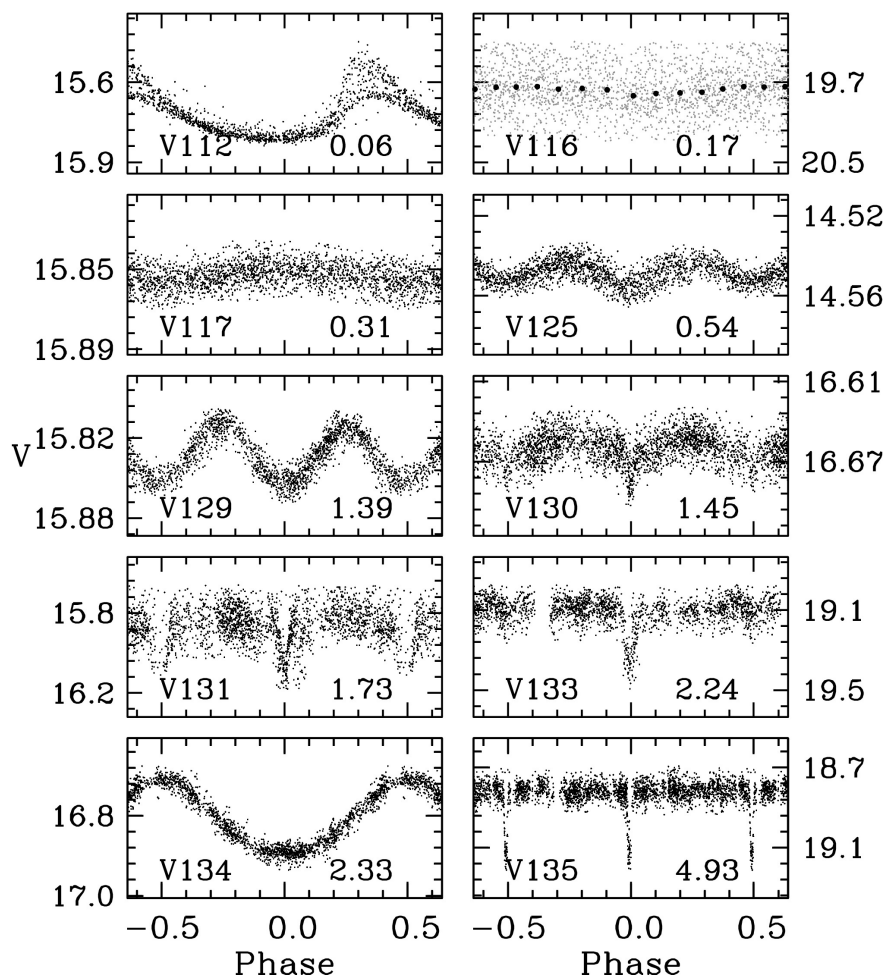


Figure 5: Phased V-band light curves for a selection of the newly detected variable members or likely members of M22. Phase-binned data are shown for V116 with heavy black points. Individual panel labels give star ID, and period in days.

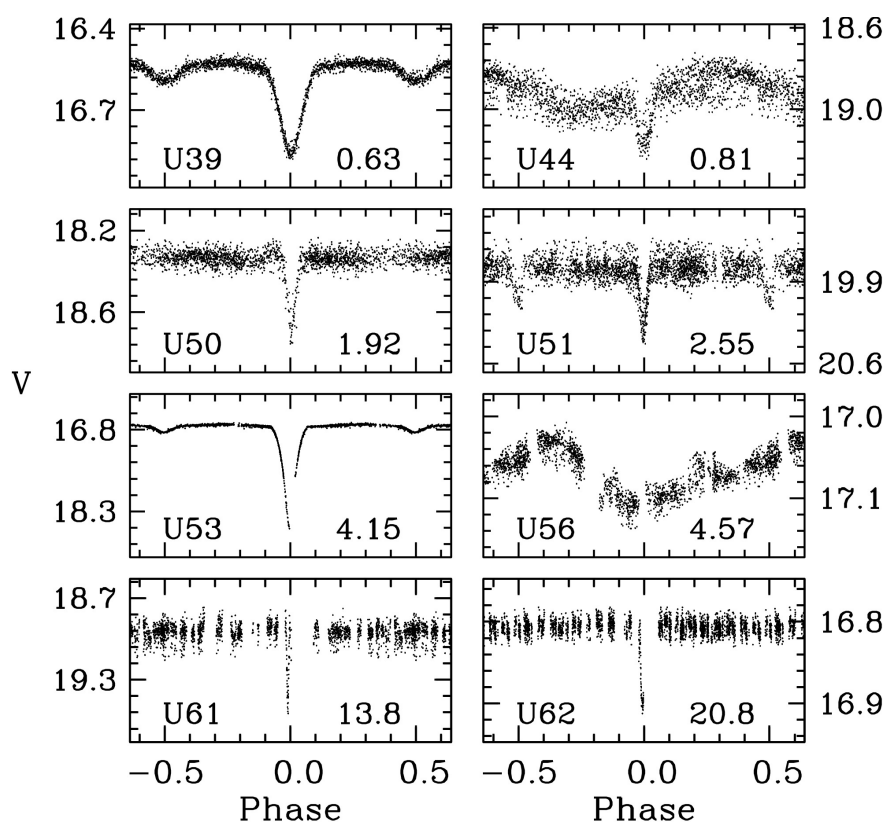


Figure 6: Phased V-band light curves for a selection of the new variables from the observed field for which no PM-data are present. Individual panel labels give star ID, and period in days.

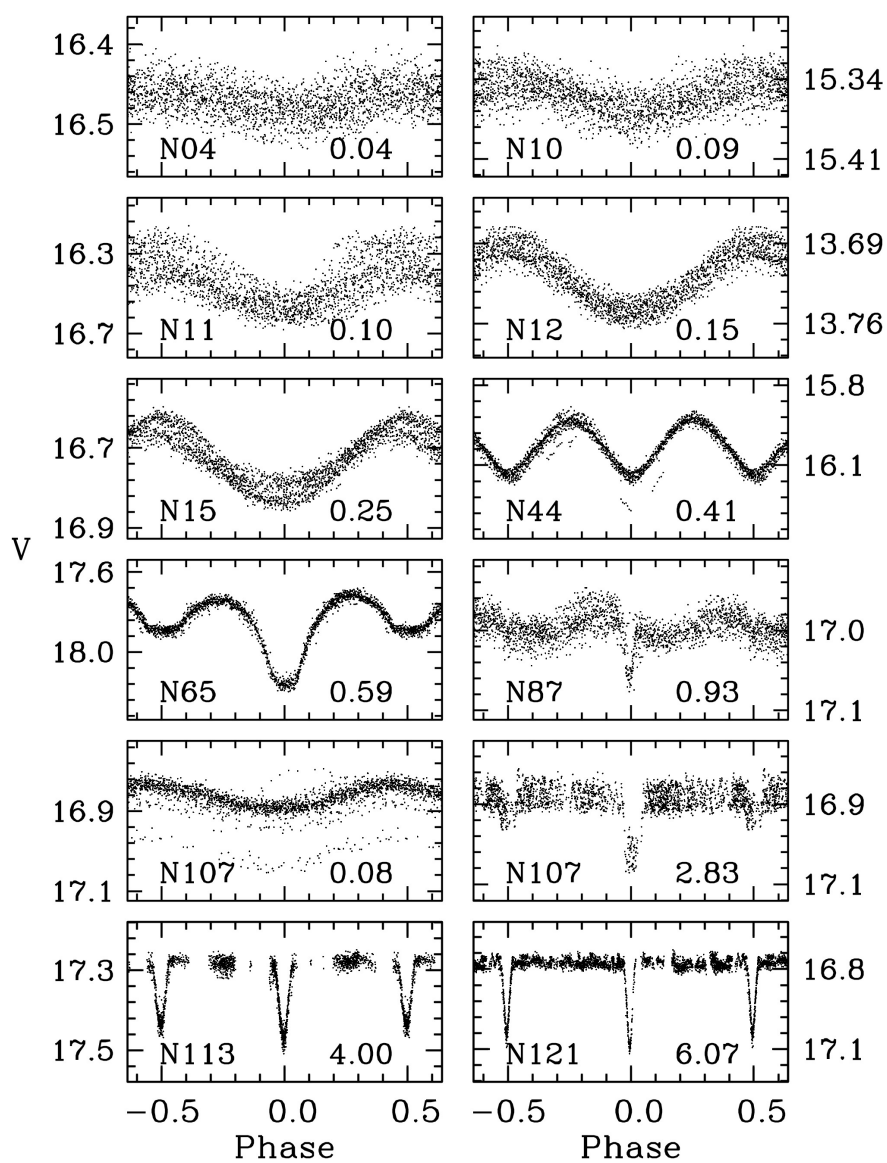


Figure 7: Phased V-band light curves for a selection of the new variables from the observed field whose proper motions indicate that they do not belong to M22. Individual panel labels give star ID and period in days. N107 is phased with the pulsation period of its  $\delta$  Sct / SX Phe component, and with the orbital period.

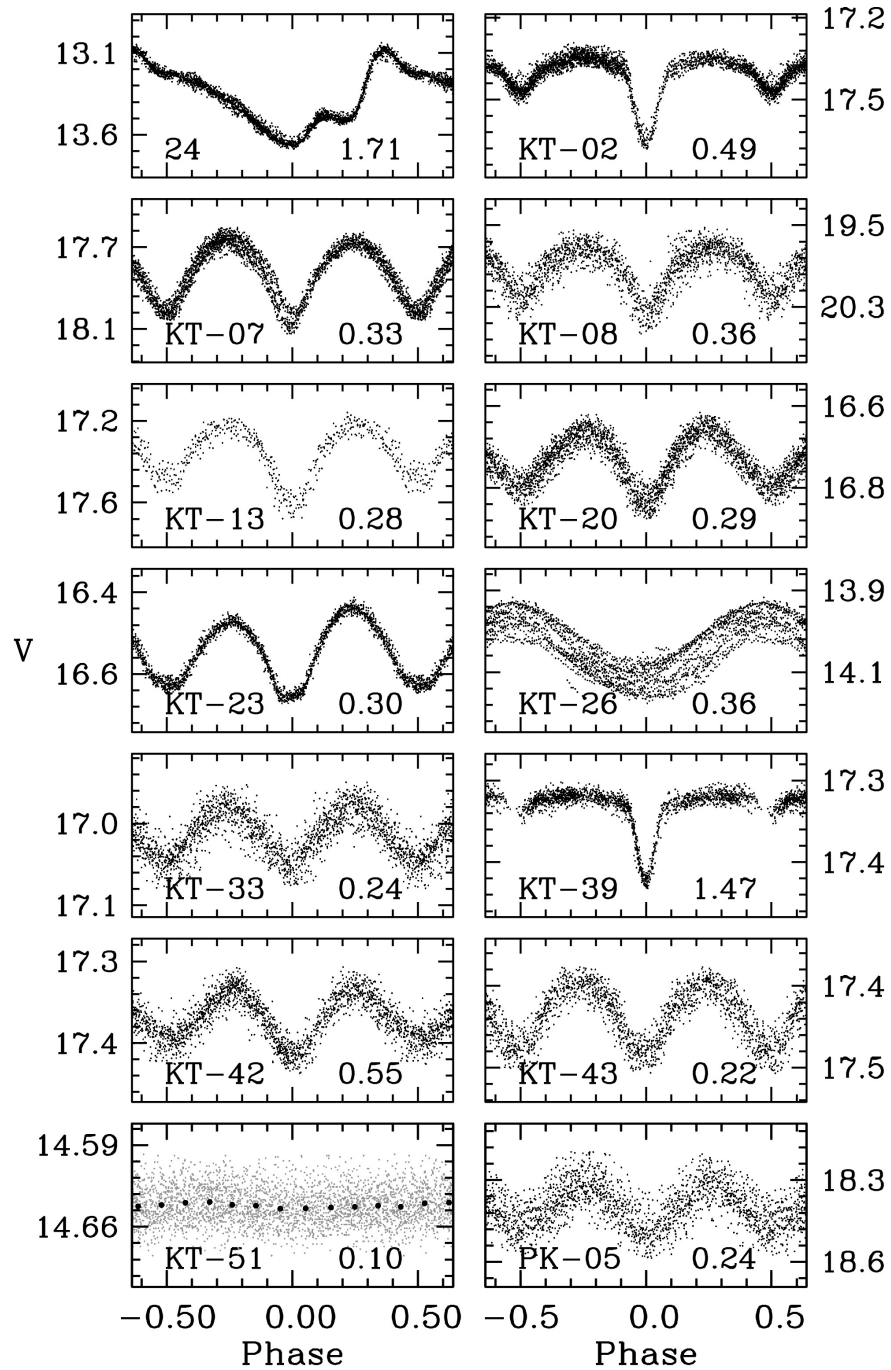


Figure 8: Phased V-band light curves for a selection of the M22 variables cataloged by C01-17. Phase-binned data are shown for KT-51 with heavy black points. Individual panel labels give star ID from the C01-17 catalog, and period in days.